Reduction of Core-loss in the High Frequency Band of the Fe-Si-Cr Crystalline Alloy According to Particle Size

Yeon Jun Choi
Hankuk University of Foreign Studies
Ji Hun Ahn
Hankuk University of Foreign Studies
Deok Hyeon Kim
Hankuk University of Foreign Studies
Ye Rae Kim
Hankuk University of Foreign Studies
Bo Wha Lee (bwlee@hufs.ac.kr)
Hankuk University of Foreign Studies

Research Article

Keywords: soft magnetic composites (SMCs), metallic alloy, permeability, high frequency

Posted Date: December 20th, 2021

DOI: https://doi.org/10.21203/rs.3.rs-1157982/v1

Abstract

In order for soft magnetic composites (SMCs) to achieve the high-performance requirements expected of them even at high frequencies, high permeability and low core-loss are required. In this study, we used different sizes of gas atomized Fe-Si-Cr alloy powder to produce SMCs, this alloy has higher resistivity than existing materials used in SMCs such as Fe-Si alloy or pure Fe. These powders were prepared by sieving raw materials which had an average size from less than 25 μm to over 63 μm. Our experiments show that as particle size decreases, the magnetic saturation tends to increase, the sample made from the powder with particles 25-38 μm in size recorded the highest magnetic saturation of 169.38 emu/g. Additionally, as particle size decreased, permeability increased. The sample made from powder with particles under 25 μm had a permeability of 20.7 H/m at 1 MHz. Also, the relationship between particle size and quality factor was found to be inversely proportional. Finally, the minimum core-loss was 187.26 kW/m^3 at 1 MHz for the sample made from powder whose constituent particles are under 25 μm. We also observed that the core-loss is proportional to particle size.

1. Introduction

Soft magnetic composites (SMCs) with high saturation magnetization (M_s), low coercivity (H_c), and low core-loss (P_{cv}) are essential for electronic devices to achieve high energy efficiency at high frequencies. [1–6] There has been a great deal of research effort directed at improving the working frequency of devices using SMCs. However, due to limitations that come with increasing the working frequency, improving DC-bias characteristics has been the method used to improve the efficiency of SMCs used in electronic devices. [7, 8] Studies related to soft magnetic materials are being actively undertaken with the goal of maintaining the stability of permeability and high-current at high frequencies over 1 MHz. [9] Recently, SMCs mixed with insulating polymer have proven to be an interesting alternative material because of the improvement they provide in overall permeability and the prevention of inter-particle eddy-current loss (P_e) they provide, which then reduces core-loss (P_{cv}). [10–12]

Fe based alloys have shown promising DC magnetic properties such as low coercivity, high magnetization saturation and high permeability. However, eddy-currents are easily generated because of Fe based alloy's relatively low resistivity, which causes high energy loss. [13] To overcome this problem, Fe based amorphous materials have been used in power applications because of their high electrical resistivity. However, amorphous materials have the drawback of low saturation flux density compared to that of silicon steel. [14] Fe-Si-Cr metallic alloys have relatively high electrical resistivity compared to Fe-Si metallic alloy, this is because of the Cr-rich oxidation layer created by Cr addition, which can result in reductions in core-loss based on decreased eddy-current loss. [15–17] Also, crystalline powders achieve higher magnetization saturation than amorphous powders while being easier to fabricate. In addition, based on Snoek's limitation, the magnetic resonance frequencies of metal powder cores occur in the MHz band, metal powder cores are considered suitable for use as electronic components in the MHz frequency range. [18, 19] For these reasons, we chose Fe-Si-Cr metallic alloy as our candidate material.

Core-loss consist of the hysteresis loss (P_h), eddy-current loss (P_e) and residual losses (P_r), as shown in equation (1).

$$P_{cv} = P_h + P_e + P_r = K_h B_m^{\beta} f + K_e \left(B_m f\right)^2 + K_r \left(B_m f\right)^{1.5}$$

1

However, in these cases the amount of residual loss is remarkably low, as such, we can ignore the contribution from residual loss. [20] In order to reduce hysteresis loss, we should use materials with soft magnetic properties, while to reduce eddy-current loss, using materials that have high resistivity is important when it comes to reduce eddy-current loss because the eddy-current loss per unit volume of a spherical iron particle can be expressed as $P_e(t) = \frac{r_{Fe}^2}{10\rho_{Fe}} \left(\frac{dB}{dt}\right)^2$, where ρ: electrical resistivity, r: radius of the particle, this relation means that improving resistivity and reducing the particle size can result in decreased eddy-current loss. [21]

In this study, we measured the magnetic properties of various Fe-Si-Cr alloys with different particle sizes. There have been no reports about how particle size affects a core's magnetic performance for Fe-Si-Cr alloys. Motivated by this, in this paper, we investigated the magnetic properties of alloy-resin composites according to the size of the particles used in each Fe-Si-Cr alloy.

2. Experimental

Fe-Si-Cr alloy powders, produced using the gas atomizing method, were commercially purchased. The Fe-Si-Cr powders were classified into one of five size ranges according to their constituent particle size using sieves with holes ranging from 25 to 63 μm wide. The powders were divided into groups of under 25 μm, 25-38 μm, 38-53 μm, 53-63 μm and over 63 μm. The sieved powders were denoted 'S1' for the under 25 μm group, 'S2' for the 25-38 μm group, 'S3' for the 38-53 μm group, 'S4' for the 53-63 μm group, and 'S5' for the over 63 μm group. In order to create a sample toroidal core with inner diameter 13 mm, outer diameter 20mm, we mixed 3.0 wt% epoxy binder with the alloy powder and pressed the mixture at a pressure of 1.5 ton at room temperature before heat treatment at 200 ℃ for 2 hours in air. Characteristics of the Fe-Si-Cr powders were measured by looking at their particle size distribution (PSD), X-ray diffraction (XRD) using Cu-K_α, scanning electron microscopy (SEM) and energy dispersive spectroscopy (EDS) measurements. The resistivity of the material was measured using a powder resistivity measurement system. The magnetic properties of the SMCs were measured using a vibration sample magnetometer (VSM) and an impedance analyzer to obtain permeability and quality factor measurements. Core-loss was measured using a *B-H* analyzer over various frequencies.

3. Result And Discussion

Table 1 shows the particle size distribution of the Fe-Si-Cr alloy powder according to D90, D50 and D10 measurements. Figure 1 shows the result of PSD for each group of the sieved Fe-Si-Cr alloy powders. We can see that the distribution in most samples is uniform. However, S5 shows quite a wide distribution, this is because all powder particles over 63 μm were included in S5 leading to a wider distribution.

Table 1
Particle size distribution of the sieved Fe-Si-Cr alloy powders

Sample	S1	S2	S3	S4	S5
D90 (μm)	35.31 μm	50.90 μm	70.64 μm	92.98 μm	140.05 μm
D50 (μm)	19.72 μm	35.23 μm	50.97 μm	63.89 μm	98.12 μm
D10 (μm)	10.03 μm	26.23 μm	39.32 μm	49.55 μm	68.52 μm

X-ray diffraction (XRD) patterns are shown in Figure 2. A Cu-K_{α} source was used for measurements taken from 20° to 90° at 0.01° intervals. After the Fe-Si-Cr alloys were divided into five groups according to fraction sizes and the XRD data was recorded, it was found that the XRD peaks appear in almost the same places as the characteristic peaks of Fe. The majority of the content in the Fe-Si-Cr alloy powders is Fe, while Si and Cr contents are relatively smaller, as such, it is natural that the XRD peaks are close to those expected from pure Fe.

Figure 3 shows the morphology of the Fe-Si-Cr alloy powder in each group. The shapes of the particles in the powders turned out to be spherical, this is because the powder was fabricated using the gas atomizing method. The S2 to S5 SEM images were recorded at ·300 and ·1,500 magnification, while the S1 was recorded at ·300 and ·2,000 magnification. Figure 4 show the energy dispersion spectroscopy (EDS) data for the sieved Fe-Si-Cr alloy powders. The EDS data shows that each sample contains about 87 wt% of Fe, about 11 wt% of Si and about 2 wt% of Cr.

In Figure 5, the field dependence of magnetization for the Fe-Si-Cr alloy powders is represented. As shown in Figure 1, S5 powder has an extremely broad distribution compared to other samples. So, we decided to exclude the S5 data because of the possibility of not enough accuracy of the data. Figure 5**(a)** shows the magnetic hysteresis loop, Figure 5**(b)** shows the enlarged hysteresis loop data from -15 to 15 Oe and Figure 5**(c)** shows the relationship between the magnetization saturation and coercivity for each particle size. When measuring the VSM for each powder size group, Fe-Si-Cr alloy was found to have soft magnetic the characteristics with low coercivity. The sample showing the highest magnetization saturation was S2 with a saturation value of 169.38 emu/g and a size of 25-38 μm, while the sample with the lowest coercivity was the 38-53 μm sample with a value of 0.93543 Oe. Generally, higher magnetization saturation induces good DC-bias characteristic, which means the inductance maintains as the current increases.[22] However, in order to induce good properties of electronic devices like powder-inductors, enhanced properties are required for not only magnetization saturation, but also permeability, resistivity, and core-loss.

Figure 6 shows the frequency dependence of each group's permeability over a frequency range from 100 kHz to 110MHz. Figure 6**(a)** and **6(b)** show the real and imaginary parts of each group's permeability, respectively, at 1 MHz and 3 MHz. Figure 6**(c)** shows the quality factor for each group of the sieved Fe-Si-Cr alloy powders. The relationship between permeability and quality factor is expressed in equation (2).

$$Q = \frac{\mu'}{\mu''} = \frac{\frac{B_0}{H_0}\cos\delta}{\frac{B_0}{H_0}\sin\delta} = \frac{1}{\tan\delta}$$

2

Quality factor is inversely proportional to the loss tangent ($\tan\delta$), which means the lower loss a sample has, the higher the quality factor is. [23] Figure 6**(d)** shows the permeability for each group at frequencies of 1 MHz and 3 MHz. The impedance analyzer shows that S1 has the highest permeability in the 1 MHz and 3 MHz bands, these are the bands mainly used by portable electronic devices. [24] Therefore, it seems that S1 would be more suitable in high frequency applications because it maintains its permeability stable in high frequency. Also, if we check the quality factor, we can see that the quality factor and resonance frequency both increase as the powder particle size decreases.

The electrical resistivity of the powder is an important physical quantity that directly affects the intra-particle eddy-current loss from the SMC core the powder is used to form. The resistivity of each powder was measured by a powder resistivity measurement system. The resistivity was measured by pressing the powder increments from 0 to 2.0 ton, with the press increasing 0.2 ton in each step. The final data expressed in Figure 7 is the data collected from the final 2.0 tons press, this is when the powder compaction density is at its greatest, this data is the closest to the actual resistivity of each powder. The S1 powder showed the highest resistivity at 0.3352 Ω•cm. So, S1 is expected to have the lowest core-loss based on highest resistivity, influenced by decrease of eddy-current loss.

In Figure 8, the core-losses from each group of Fe-Si-Cr powders according to frequency is presented. The core-losses of the Fe-Si-Cr cores were measured at a fixed value of B_m = 10 mT. Figure 8**(a), (b)** and **(c)** show how the core-loss, hysteresis loss and eddy-current loss increase linearly with the particle size of the Fe-Si-Cr alloy powders. Hysteresis loss and eddy-current loss were separated from the total core-loss using curve fitting. Figure 8**(d)** shows the core-loss, hysteresis loss and eddy-current loss of each sample measured at 1 MHz. The S1 powder, which has the smallest particle size, showed the lowest core-loss of 187.26 kW/m^3 at 1 MHz. The graph shows that the decrease in hysteresis loss is smaller than the decrease in eddy-current loss as the particle size decreases. This means that the total core-loss of the samples is dominated by the eddy-current loss rather than the hysteresis loss. These results come from the intrinsic properties of Fe based materials, where increased eddy-current loss is a major factor in the increased total core-loss at high frequency. As such, the increased core-loss in the large size powders is because of an increase of eddy-current loss caused by intra-particle eddy currents. [25, 26] The

relationship between the resistivity and core-loss shows that group with high resistivity also had low core-loss because of the reduction in intra-particle eddy-current loss.

4. Conclusion

In this study, the permeability, Q-factor, and core-loss dependency of various cores were investigated, these cores were made from Fe-Si-Cr metallic alloy powders that were grouped according to their constituent particle size. Changes in permeability according to the particle sizes of the samples were found, it was also found that core-loss varies with particle size. In order to produce a SMC with good magnetic properties in the high frequency domain, it is necessary to use the appropriate particle size when fabricating the core as this affects both the magnetic permeability and core-loss which are both critical factors in achieving high efficiency at high frequencies. As a result of our investigation, we found that cores composed of powder made up of particles that are only few tens of a μm show stable AC magnetic properties and low core-loss. Particularly, in our study, the S1 sample made from particles less than 25 μm in size showed the lowest core-loss of 187.26 kW/m^3 based on this sample having the highest electrical resistivity, this shows that samples made from small sized particles are good candidates for high-frequency power-inductor applications.

Declarations

ACKNOLEDGEMENTS

This research was supported by Materials, Components & Equipment Research Program funded by the Gyeonggi Province (AICT-003-T1).

CONFLICT OF INTEREST

The authors declare that they have no known competing financial interests or personal relationships that could have appeared to influence the work reported in this paper.

References

1. J.M Silveyra, E. Ferrara, D.L. Huber, and T.C. Monson, *Science*, **362**, 418 (2018)
2. W. Li, H. Cai, Y. Kang, Y. Ying, J. Yu, J. Zheng, L. Qiao, Y. Jiang, and S. Che, *Acta Mater.*, **167**, 267–274 (2019)
3. K.J. Sunday, and M.L. Taheri, *Met. Powder Rep.*, **72**(6), 425 (2017)
4. Q. Zhu, L. Li, M.S. Masteller, and G. J. Del Corso, *Appl. Phys. Lett.*, **69**, 3917–3915 (1996)
5. A. Makino, *IEEE Trans. Magn.*, **48**, 1331–1335 (2012)
6. A. Talaat, M.V. Suraja, K. Byerly, A. Wang, Y. Wang, J.K. Lee, and P.R. Ohodnicki Jr, *J. Alloys Compd*, **870**, 159500 (2021)

7. T. Shafer, Power Inductors 101, *Vishay Technical Note*, 34450 (2017)
8. C.A. Baguley, B. Carsten, and U.K. Madawala, IEEE Trnas. Magn., **44**(2), 246–252 (2008)
9. A. Goldman, 'Handbook of Modern Ferromagnetic Materials', *Kluwer Academic Publishers*, Boston, USA, p.183 (1999)
10. T. Saito, S. Takemoto, and T. Iriyama, *IEEE Trans. Magn.*, **41**, 3301–3303 (2005)
11. T. Saito, and S. Takemoto, *J. Jpn. Soc. Powder and Powder Metall.*, **52**, 571–575 (2005)
12. B.V. Velamakanni, and F.F. Lunge, *J. Am. Ceram. Soc.*, **74**, 166–172 (1991)
13. I. Kowase, T. Sato, K. Yamasawa, and Y. Miura, *IEEE Trans. Magn.*, **41**(10), 3991–3993 (2005)
14. H.R. Lashgari, D. Chu, S. Xie, H. Sun, M. Ferry, and S. Li, *J. Non. Crys. Solids*, **391**, 61–82 (2014)
15. H.I. Hsiang, J. Mater. Sci. Mater. Electron., **31**, 16089–16110 (2020)
16. Matsuura, H.Otake, K. Magnetic material and coil component using the same. U.S. Patent 8 416 051, B2, 27 April 2011
17. T.D. Zhou, J.K. Tang, and Z.Y. Wang, *J. Magn. Magn. Mater.*, **322**(17), 2589–2592 (2010)
18. T. Ueno, H. Tsuruta, T. Saito, A. Watanabe, T. Ishimine, and K. Yamada, *SEI Tech. Rev.*, **82**, 9–15 (2016)
19. J.L. Snoek, *Physica*, **14**(4), 207–217 (1948)
20. H. Shokrollahi, and K. Janghorban, *J. Mater. Proc. Tech.*, **189**, 1-12 (2007)
21. A.H. Taghvaei, H. Shokrollahi, K. Janghorban, and H. Abiri, *Mater. Des.*, **30**, 3989–3995 (2009)
22. G. Herzer, *IEEE Trans. Magn.*, **26**(5), 1397–1402 (1990)
23. Z.H. Khan, M.M. Rahman, S.S. Sikder, M.A. Hakim, and D.K. Saha, *J. Alloys Compd.*, **548**, 208–215 (2013)
24. J.G. Yeo, D.H. Kim, Y.J. Choi, and B.W. Lee, *J. Electron. Mater.* **48**(9), 6018–6023 (2019)
25. S. Konda, Y. Yoshida, and O. Ichinokura, *AIP Adv.* **7**, 056678 (2017)
26. H. Kim, and S.Y. An, *J. Magn.*, **20**(2), 138–147 (2015)

Figures

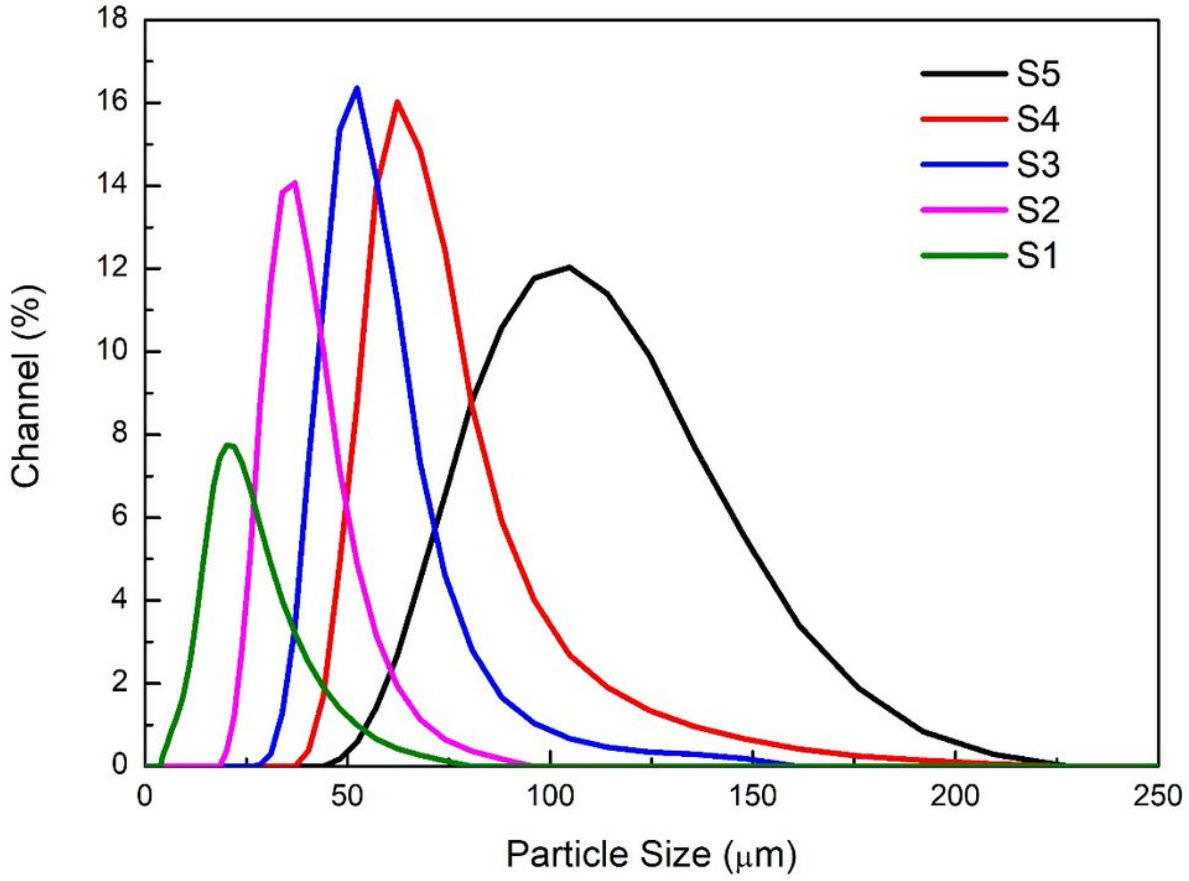

Figure 1

Particle size distribution of the sieved Fe-Si-Cr alloy powders

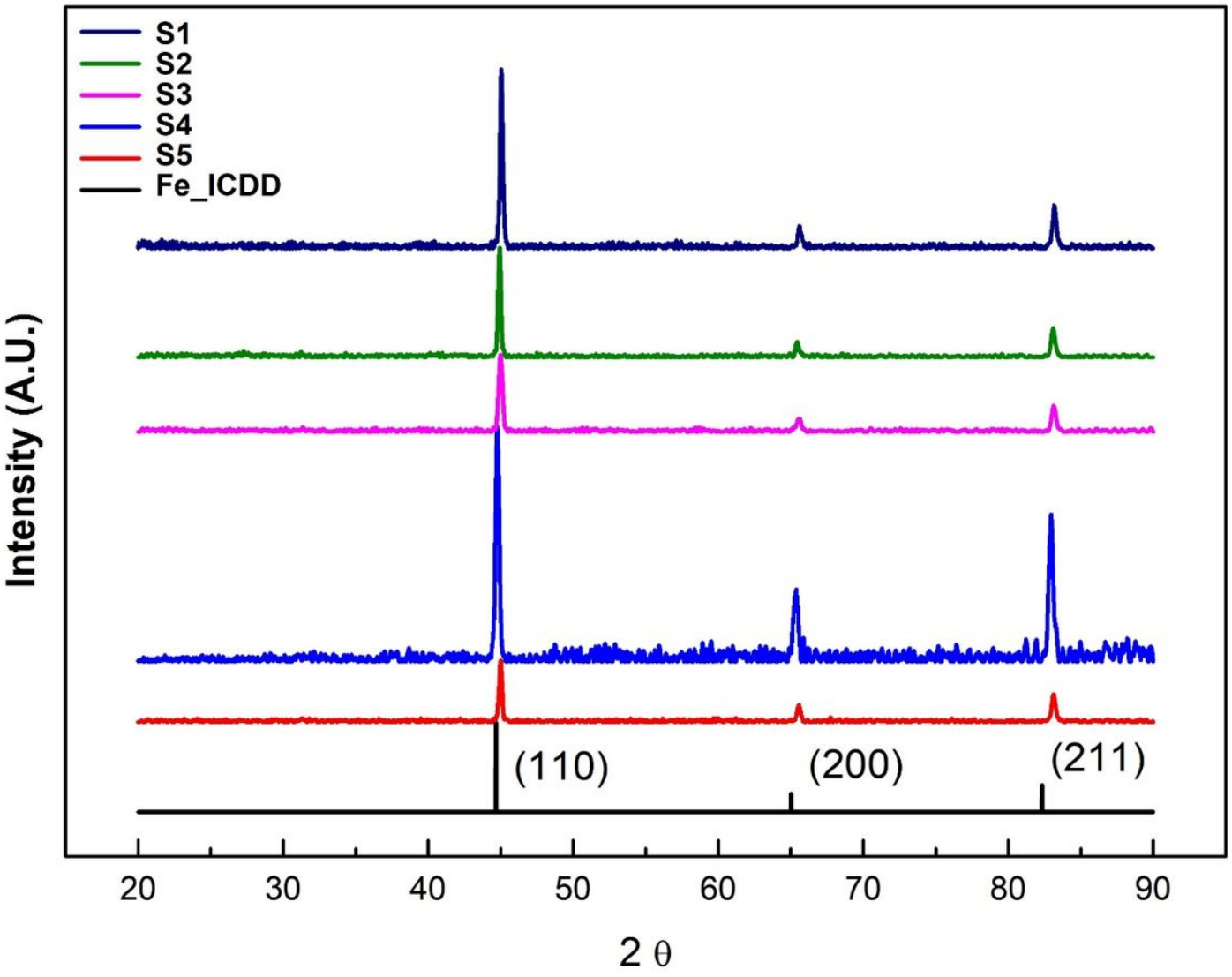

Figure 2

X-ray diffraction patterns of the sieved Fe-Si-Cr alloy powders

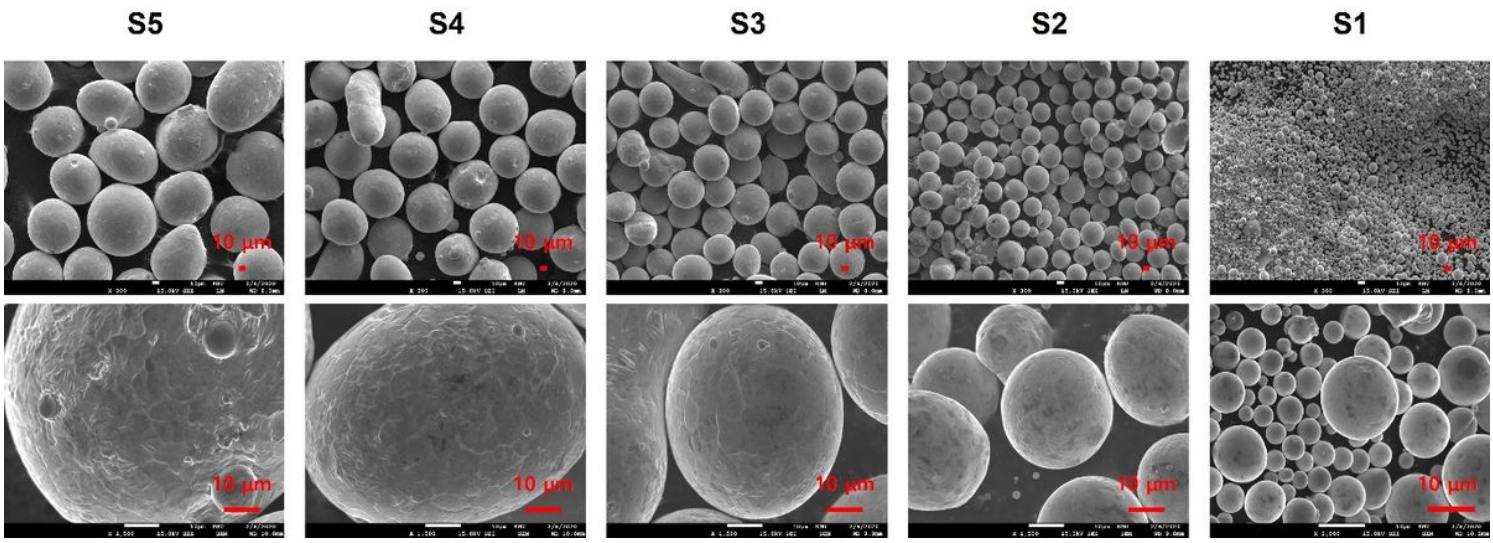

Figure 3

The morphology of the sieved Fe-Si-Cr alloy powders

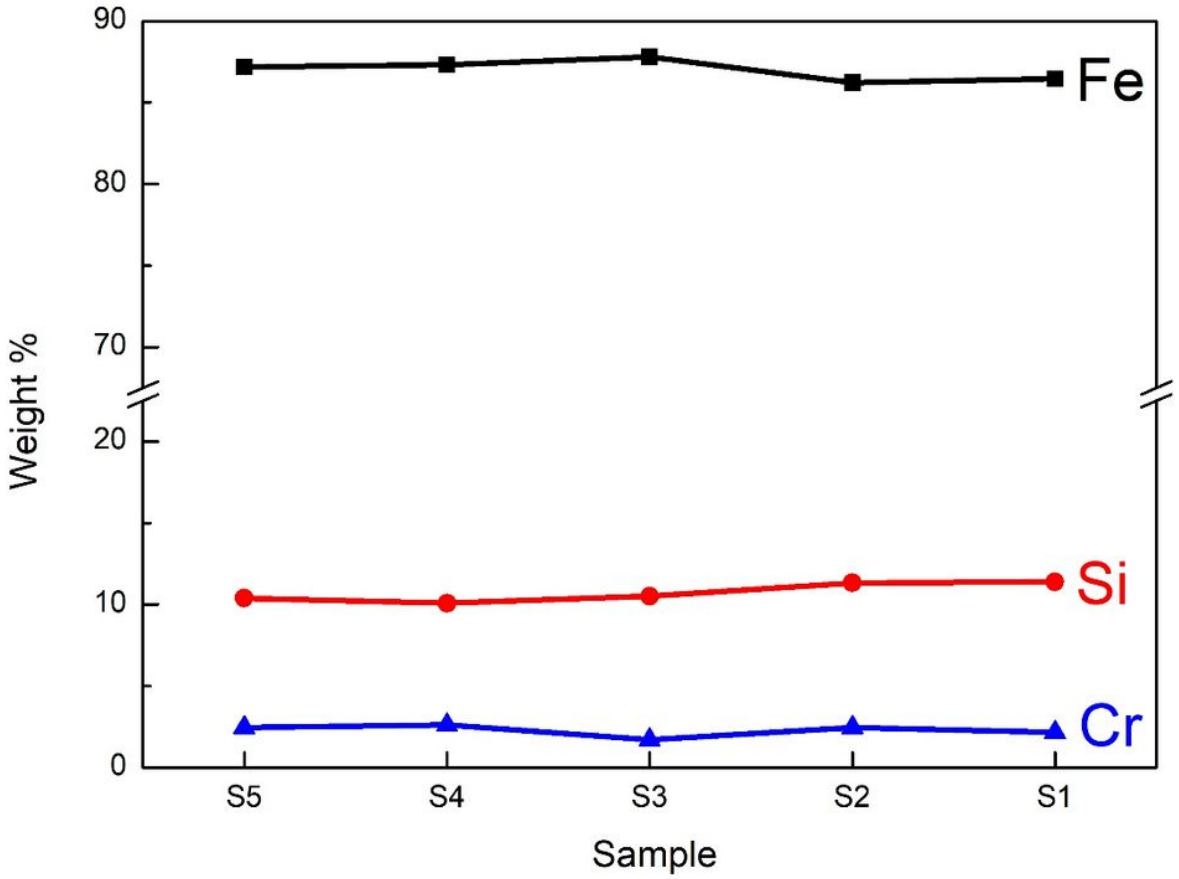

Figure 4

Weight percentages of Fe, Si and Cr in each group of sieved Fe-Si-Cr alloy powder

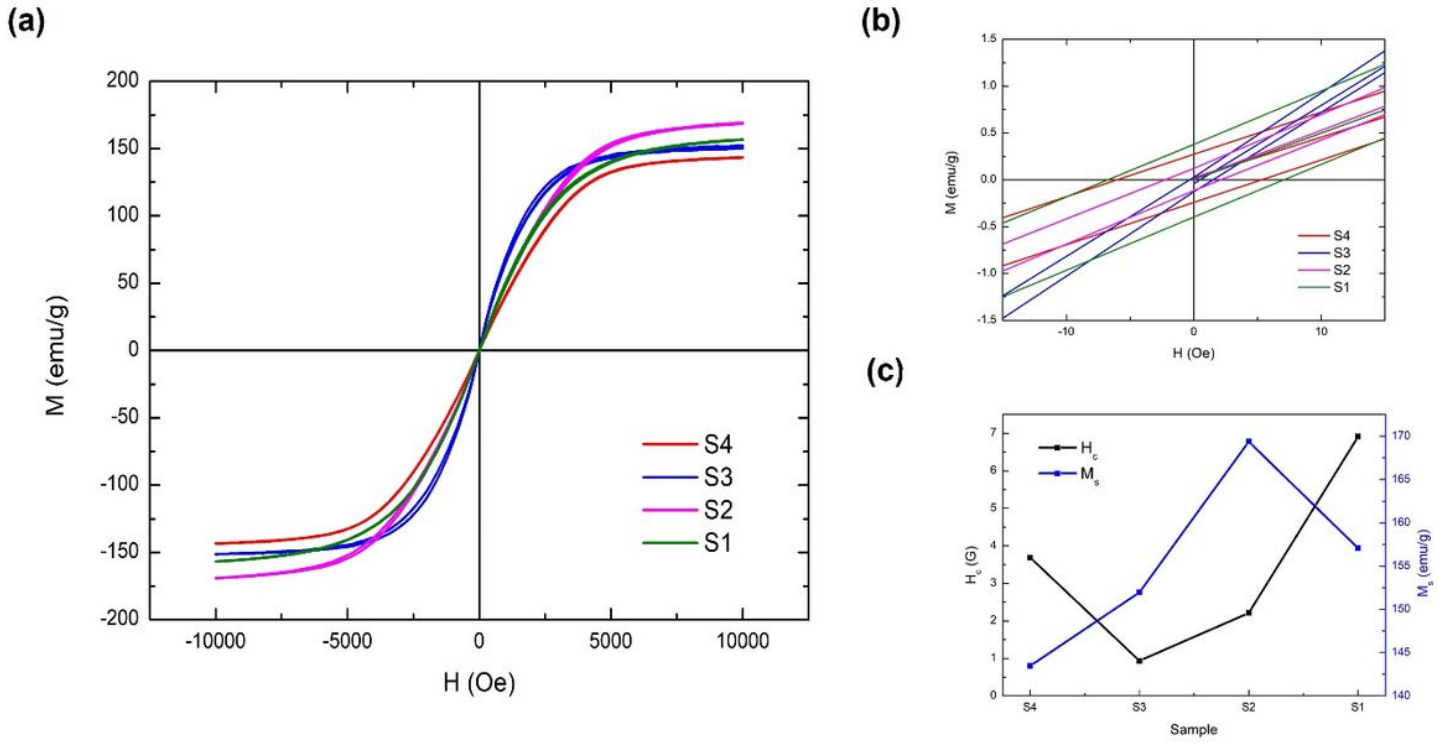

Figure 5

(a) The magnetic hysteresis loop (b) The enlarged data from -15 to 15 Oe (c) The magnetization and coercivity of the Fe-Si-Cr alloy powders

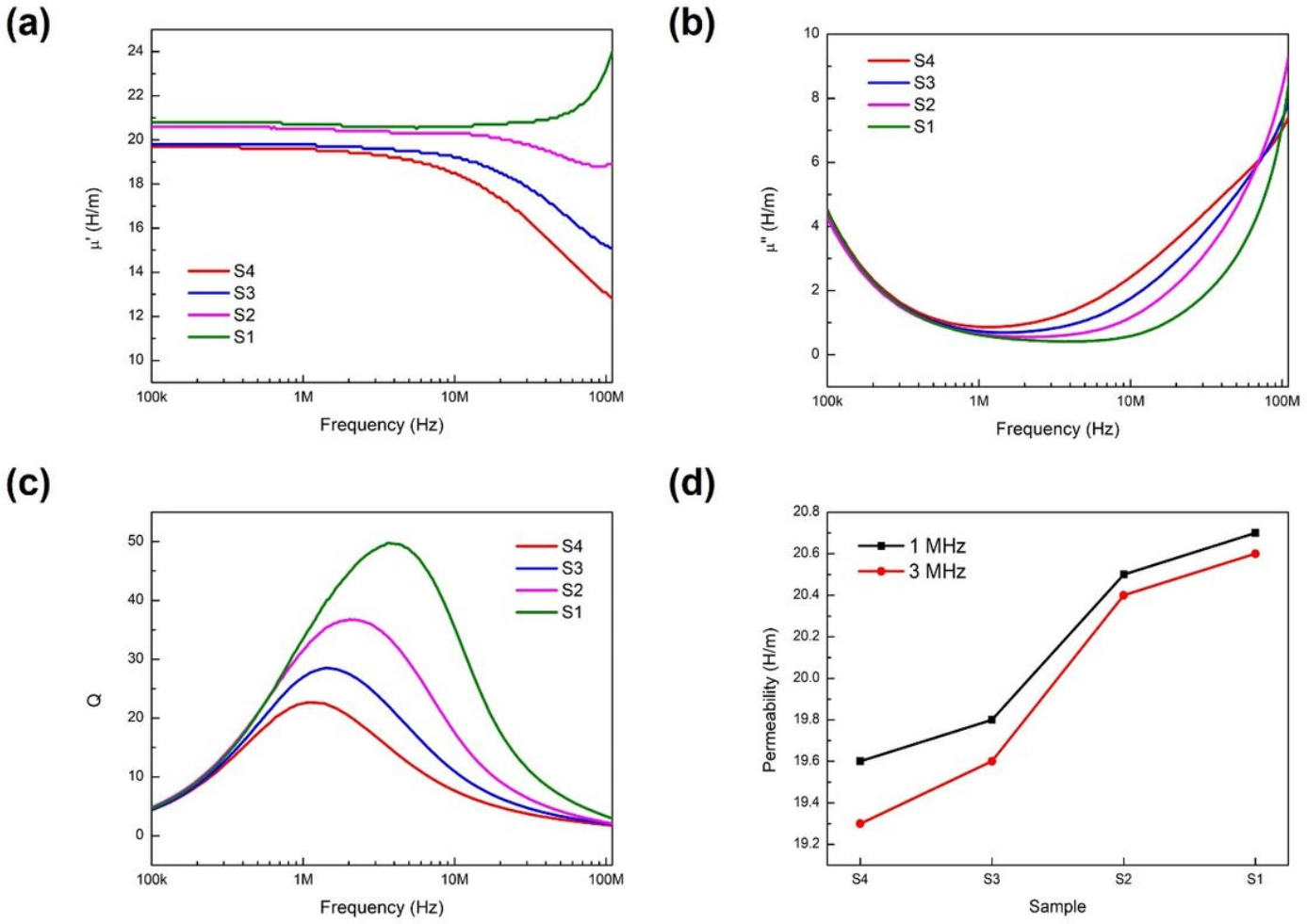

Figure 6

(a) Real part of permeability (b) Imaginary part of permeability (c) quality factor as a function of applied frequency from 1 kHz to 110 MHz (d) permeability for each group at 1 MHz and 3MHz

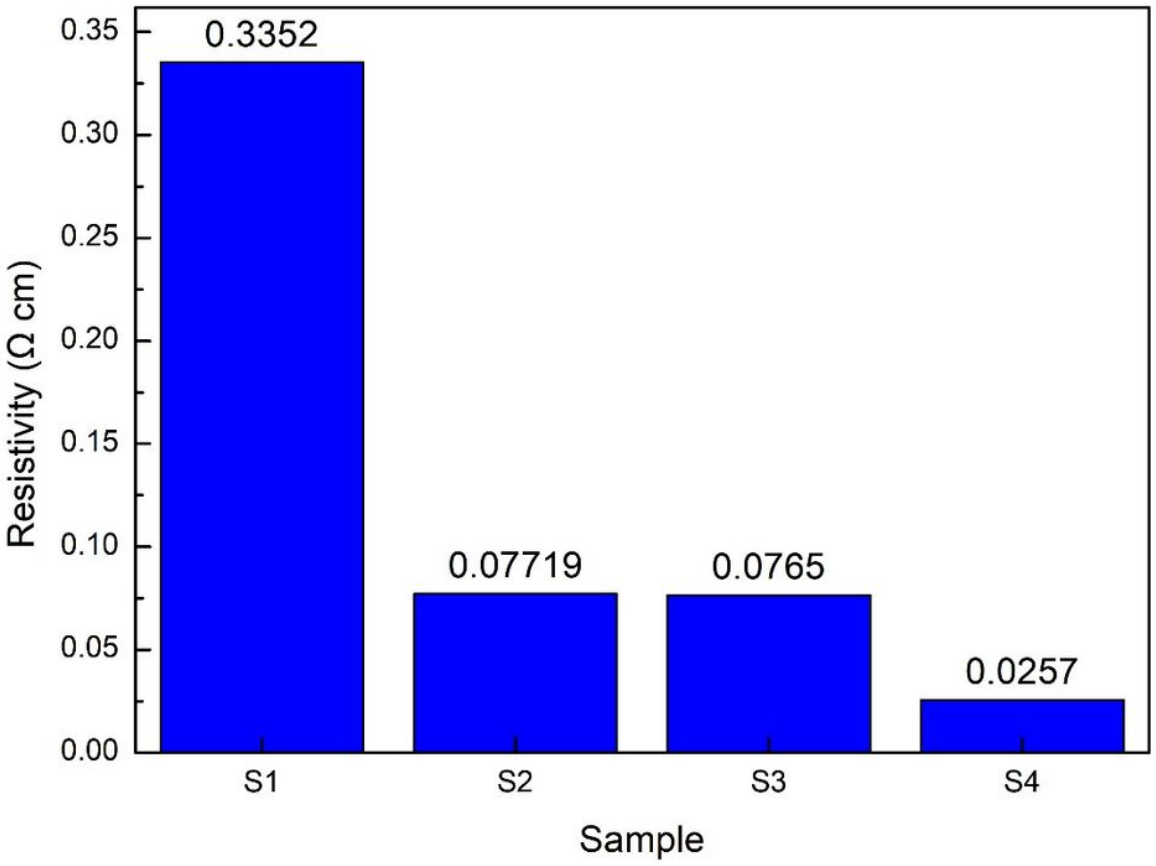

Figure 7

Powder resistivity according to the particle size of the sample

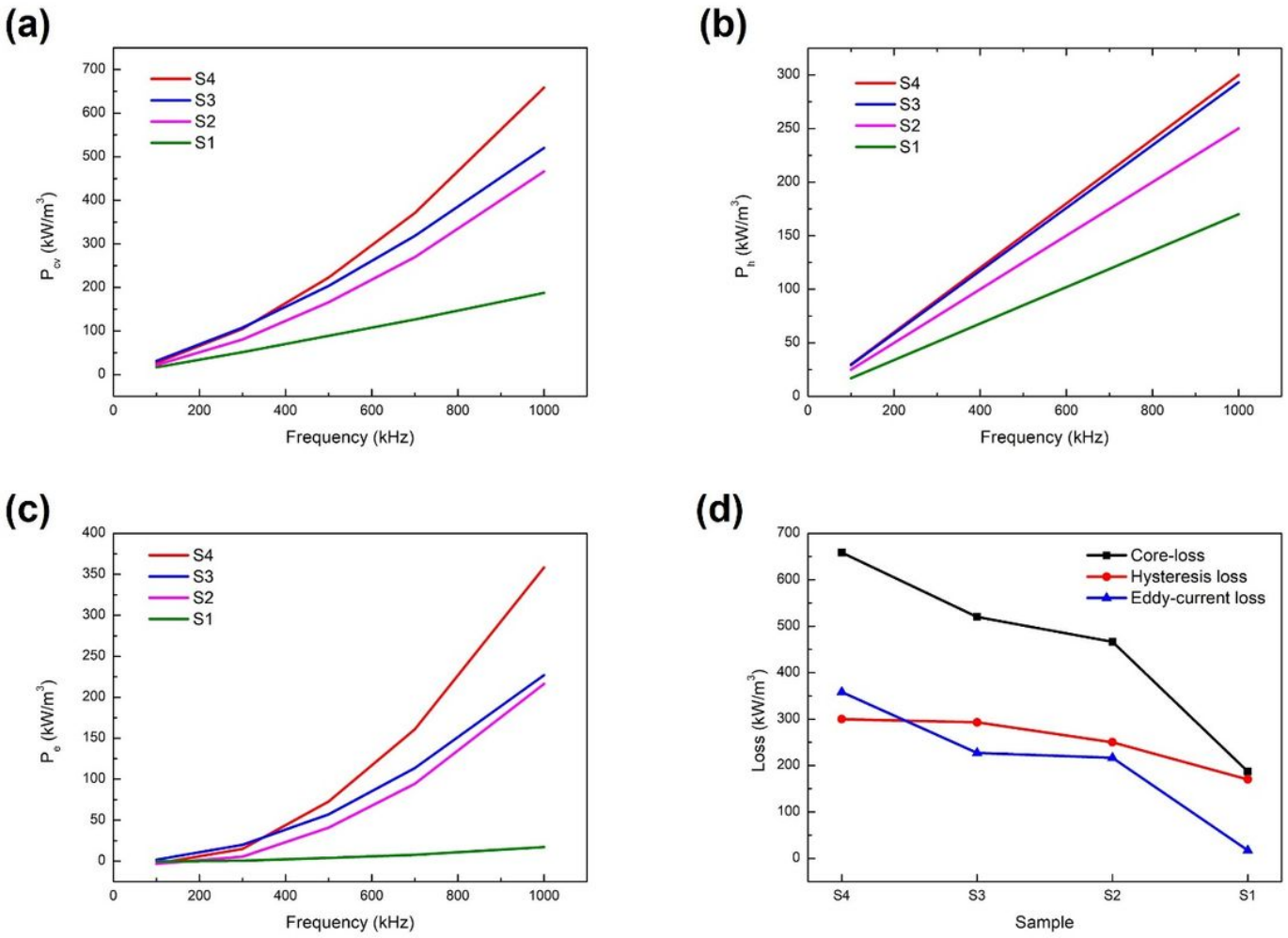

Figure 8

(a) The total core-loss, **(b)** hysteresis loss, **(c)** eddy-current loss of each group measured from 100 kHz to 1 MHz **(d)** the measured loss at 1 MHz of each sample